Supporting Information for

"Improving Coral Paleoclimate Reconstructions using Paired Geochemistry and Density Records: A Case Study from the Galápagos Islands"

E. V. Reed[1], D. M. Thompson[1], J. E. Cole[2], J. M. Lough[3,4], N. E. Cantin[3], Anson Cheung[5], Alexander Tudhope[6], Lael Vetter[1], Gloria Jimenez[7], and R. Lawrence Edwards[8]

[1]Department of Geosciences, 1040 E. 4th St., University of Arizona, Tucson, AZ 85721

[2]Department of Earth and Environmental Sciences, 1100 N. University Ave., University of Michigan, Ann Arbor, MI 48109

[3]Australian Institute of Marine Science, PMB 3, Townsville MC, Queensland 4810, Australia

[4]ARC Centre of Excellence for Coral Reef Studies, James Cook University, Townsville, Queensland 4811, Australia

[5]Department of Earth, Environmental, and Planetary Sciences, Brown University, Providence, RI 02912

[6]School of Geosciences, University of Edinburgh, Edinburgh, UK

[7]Chubb Limited, Philadelphia, PA, 19106

[8]Department of Earth Sciences, University of Minnesota, Minneapolis, MN

Contents

S1. Geochemical Methods

Geochemistry was measured using a Jobin-Yvon (JY) Optima 2c inductively coupled plasma atomic emission spectrometer (ICP-AES) and a Thermo iCAP 7400 series ICP-AES, both at the University of Arizona. The instrument used for each coral record is given in Table S1. Powder samples (0.35-0.45 mg for JY data; 0.50-0.70 mg for iCAP data) were acidified in 3.5 mL of 5% trace metal grade HNO_3 to achieve a dilution of approximately 80 ppm Ca, and trace element ratios were measured [after *Schrag*, 1999]. The wavelengths used for measuring each trace element differed between instruments. JY data was measured using Sr (407 nm)/Ca (393 nm) and Mg (285 nm)/Ca (393 nm); for iCAP data, Sr (421.552 nm)/Ca (315.887 nm) and Mg (280.270 nm)/Ca (315.887 nm) were measured with a radial torch view, and Ba (455.403 nm)/Ca (370.603 nm) was measured with an axial view. Plasma drift

Corresponding author: E. V. Reed, evreed@email.arizona.edu

was first corrected by using a reference solution of an internal coral standard, Mafia Coral Powder (MCP), dissolved in HNO_3 to achieve a Ca concentration of 80 ppm. This reference solution was measured between each coral sample; matrix effects were then corrected using a series of matrix standards with the same trace element:Ca ratio, and with Ca concentrations ranging from 40 to 70 ppm for the iCAP runs, and from 60 to 100 ppm for JY runs [*Schrag*, 1999]. For JY data, we corrected these matrix effects using a polynomial fit; for iCAP data, a linear fit was used. The relative standard deviation of the corrected matrix standards for Sr/Ca was <0.7% (typically 0.2-0.3%), and <2% for Mg/Ca and Ba/Ca. Finally, each run was standardized to the mean of repeated measurements of an internal standard, liquid MCP (MCP-L). Across all JY runs, MCP-L averaged 9.02±0.045 mmol/mol for Sr/Ca, and 4.97±0.270 mmol/mol for Mg/Ca; across all iCAP runs, Sr/Ca was 8.79±0.072 mmol mol, Mg/Ca was 5.85±0.226 mmol/mol, and Ba/Ca was 3.21±0.311 μmol/mol. An additive (linear) correction between the measured and known values of MCP-L was used for all trace elements. After the generation of WLF03 and WLF10 Sr/Ca and Mg/Ca, the Sr/Ca, Mg/Ca, and Ba/Ca values of MCP were measured on an ICP-MS in 2017 at the University of Western Australia (Advanced Geochemical Facility for Indian Ocean Research, PI: Malcolm McCulloch). These updated known MCP values were used to correct all subsequently collected data, including all data for WLF04 and 05, and Ba/Ca for WLF10. We also re-corrected WLF04 and WLF05 JY data to the new known MCP values, so that each trace element record for each core uses the same MCP known value throughout. This update may result in offsets between data corrected to old (WLF03 and WLF10 Sr/Ca and Mg/Ca, from *Jimenez et al.* [2018]) and new (all other data) MCP values; the new values differ by -0.05 and -0.15 mmol/mol from the previous values for Sr/Ca and Mg/Ca, respectively. Analytical precision for each coral record was calculated from the standard deviation of repeated measurements of powdered MCP, and are given in Table S1. For all iCAP runs, an inter-laboratory reference coral powder (JCp-1) [*Hathorne et al.*, 2013] was also measured for comparison. The long-term means of these JCp-1 values were 8.85 ±0.035 mmol/mol for Sr/Ca (mean±1σ), 3.93 ±0.138 mmol/mol for Mg/Ca, and 6.65 ±0.314 μmol/mol for Ba/Ca. These values differ from the inter-lab average value of JCp-1 by +0.01 mmol/mol, +0.27 mmol/mol, and -0.81 μmol/mol, respectively [*Hathorne et al.*, 2013].

For WLF04, the full CT1 and CT2 transects were run on both JY and iCAP instruments. Data were screened for outliers (Text S2), but with a more stringent 1σ threshold to minimize the influence of outliers on means (used in calculating the offset), yielding 197

quality-controlled samples. We observed offsets in Sr/Ca (0.02 mmol/mol) and Mg/Ca (0.40 mmol/mol) between instruments (note that Ba/Ca data was not collected on the JY), even though results from both instruments were corrected to the same known values of MCP (Fig. S4). Other studies have observed such offsets in trace elemental ratios between ICP-AES and other instruments, possibly due to spectral interference on the ICP-AES with other elements within complex coral lattices [*Cantarero et al.*, 2017]. Alternatively, this offset could result from the use of different channels between instruments. These mean differences are not observed in WLF10 JY and iCAP data (Fig. S7), possibly due to updated instrumentation between the WLF04 JY data (run in 2010-2011) and WLF10 JY data (run in 2014-2015). We tested a multiplicative ("stretch") correction, defined as the average iCAP data divided by the average JY data over the overlapping sections, as well as an additive (linear) correction of the JY data to better match iCAP results. We found that a simple additive offset produced the smallest absolute differences between the two instrumental datasets. For Mg/Ca (the elemental ratio with the largest instrumental offsets), the additive correction results in a mean absolute difference of 0.07 mmol/mol; for Sr/Ca, the absolute difference is 0.02 mmol/mol. Both fall within the analytical precision (1σ) for WLF04 (Fig. S4). This additive offset was then applied to all WLF04 JY transects (AT1, BT1, BT3).

For all cores, geochemical outliers were identified and removed prior to age modeling. An outlier was defined as a sample that was outside of the 2σ analytical precision of Sr/Ca or Mg/Ca compared to the adjacent two samples, where the adjacent two samples are within 2σ analytical precision of each other (i.e., the data are not on a strong slope). Where both Sr/Ca and Mg/Ca for one sample are identified as outliers, the Ba/Ca from the same sample was categorized as an outlier as well. Ba/Ca was not independently screened for outliers, because strong Ba/Ca signals beyond this 2σ threshold were often observed to occur on scales of 1-2mm (1-2 samples)–likely associated with upwelling variability (as in *Shen et al.* [1992])–and could be falsely identified as outliers.

S2. X-ray Densitometry Methods

X-ray densitometry was performed at the Australian Institute of Marine Science (AIMS) Coral Core Technical Workshop following the AIMS standard operating procedure. X-rays were produced using an EcoRay Orange 1040HF X-ray machine and a 16-bit iCR3600 Digital X-Ray CR scanner with single 60kV 20 mAs exposures. Corals were positioned 2.3 m directly below the X-ray source to minimize density variations due to the inverse square law

and heel effect, with seven standards located near the center/coral cores and in an identical position for each exposure. Cores were imaged in sections to avoid density measurements near the plate edges (ensuring a border of ≥2 cm at all times). The six standards were comprised of compressed *Porites* skeletal powder buttons with measured densities that range from 2.4060 to 2.4241 g cm^{-3} and a range of thicknesses (1.55 mm-7.45 mm, or 9.92 mm in the case of the densest and thickest slabs). These standards were selected to produce optical densities (i.e., grayscale values) that encompassed beyond the full range of optical density observed for each coral slice. An additional compressed *Porites* standard with thickness (6.86 mm) and density (2.3977 g cm^{-3}) similar to that of the coral samples was used as an unknown and functioned as quality control between each individual X-ray. The X-ray software was customized to produce uncompressed, raw iCR files, which are then converted to TIFF images and imported to Fiji (ImageJ) [*Schindelin et al.*, 2012] for processing and densitometry. For each set of X-rays, an image of a blank X-ray plate was taken using the same settings. This blank was then subtracted from the coral X-rays to correct for spatial homogeneity in X-ray intensity. This corrected image was then inverted to produce an X-ray positive (darker = denser), and the scale of each image was set to 200 px/cm.

Coral slice thickness was measured using a Mitutoyo Absolute digital micrometer with a precision of ±0.01 mm, which was mounted on a custom-built manual screw-driven sliding table. Each coral slice was fixed to the sliding table with the desired density transect aligned along the axis of the micrometer. We measured the thickness of the coral skeletal slice at 0.125 cm intervals along the length of each density transect, with at least one replication, and calculated mean thickness at each interval. Mean thickness measurements were then interpolated from 0.125 cm to 0.005 cm to match the sampling resolution of X-ray density.

For each transect, optical density (OD), with gray values (GV) from 0 (black) to 255 (white), was measured along 4 mm wide transects at 0.005 cm intervals. The OD of each standard was measured as the average OD of a rectangular area spanning the center each disc. We calibrated each X-ray by applying a linear fit to the natural log of each standard's mean OD versus the standard's known density × thickness (in g/cm^2) (Fig. S5). The correlation coefficients (r^2) of these calibrations consistently exceeded 0.99. The density at each 0.005 cm interval along each transect was then calculated as: $D = \frac{\frac{\ln(OD)-b}{m}}{t}$, where D is the density (g/cm^3), OD is the optical density (in GV) at a given point in the coral transect, b is the intercept (in ln(GV)) of the calibration, m is the slope (in ln(GV)/(g/cm^2)) of the calibration, and t is skeletal slice thickness (cm) at that point.

The quality control standard was within 1.6% of its known value for WLF04 and WLF05, and within 2.8% of its known value for WLF03 and WLF10. Slice thickness was 1.012±0.043 cm (mean±1σ) for WLF03, 1.001±0.033 for WLF10, 0.521±0.040 for WLF04, and 0.556±0.045 for WLF05.

X-ray density was verified by comparing to gamma density for WLF04 and WLF05. Gamma density was measured every 0.254 mm along each transect using a gamma densitometer with a 4 mm beam width [*Chalker and Barnes*, 1990]. For gamma densitometry, slice thickness was reinterpolated to 0.0254 cm accordingly.

S3. Growth metric uncertainty calculations

The uncertainty in X-ray density measurements was computed using the 1σ uncertainty in the calibration slope and intercept. The end members of this 1σ uncertainty calibration (steepest slope and highest intercept; shallowest slope and lowest intercept) were used to compute the 1σ error bounds of each density time series.

The uncertainty in extension rate was calculated from the histogram of months during which the maximum SST occurred (Fig. S2). Because this histogram was not normally distributed, a non-parametric approach was selected to estimate the probability density function of the random variable (extension) across x bins (months). A triangle kernel distribution was fitted to the histogram, and the cumulative distribution function (CDF) of this kernel was calculated as the sum of probabilities from $x = 0$ (January) to $x = 11$ (December). The 1σ uncertainty in the SST maximum was then calculated as the x-values 34.1% above and below the median CDF value (such that ± 1σ ≅ 68.2% of the distribution). This approach yields a lower-bound and higher-bound estimate of 1σ uncertainty, in months, of each individual SST maximum used as the age-model tie point. Because extension rate is calculated as the distance between two successive SST maxima, the sum of these lower-bound and higher-bound 1σ uncertainties was used as the chronological uncertainty of each extension value. Given lower-bound and upper-bound uncertainties of 1.12 and 1.36 months, respectively, the total uncertainty for each extension rate value was 2.48 months. The 1σ uncertainty in extension rate (σ_E), in cm/yr, is then given by the equation:

$$\sigma_E = \frac{12E}{12 \pm 2.48} - E$$

where E is the extension rate, in cm/yr. Given an extension rate of, say, 1.2 cm/year (that is, 1 mm/month), this equation yields extension rate uncertainties of -0.206 and 0.313 cm/yr. These uncertainties translate to a percent error of -17% and 26%, respectively.

The uncertainty in calcification rate is calculated using the uncertainties from extension rate and density. These errors violate two key assumptions in commonly used propagation of error calculations [*Ku*, 1966]: extension rate errors are large relative to extension rate values, and both density and extension rate errors are non-Gaussian. Instead, we calculate a low-end calcification rate error bound by multiplying the lower-bound 1σ density by the lower-bound 1σ extension rate. We follow a similar procedure for calculating high-end calcification rate. This approach yields a conservative estimate of calcification error.

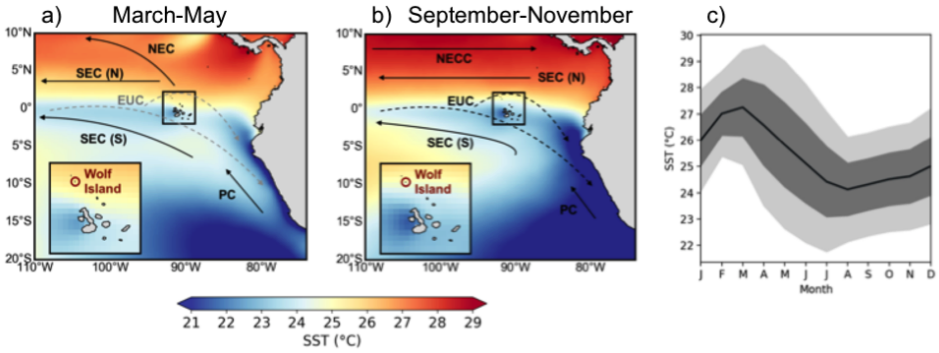

Figure S1. Climatological mean SST (OISSTv2 AVHRR 1981-2017) during: (a) the peak of the Galápagos warm season (March-May), and (b) the peak cool season (September-November). Inset: the Galápagos Islands, with Wolf Island circled. Major currents are denoted by arrows (after *Kessler* [2006]): the North Equatorial Current (NEC), South Equatorial Current North/South (SEC N/S), North Equatorial Counter Current (NECC), Peru Current (PC), and Equatorial Undercurrent (EUC, dashed gray lines). Subsurface currents are marked with dashed lines; the seasonal weakening of the EUC is shown in gray. (c) Climatological monthly mean SST for Wolf Island (1-1.5°N, 268-269°E), with 1σ (dark gray) and 2σ (light gray).

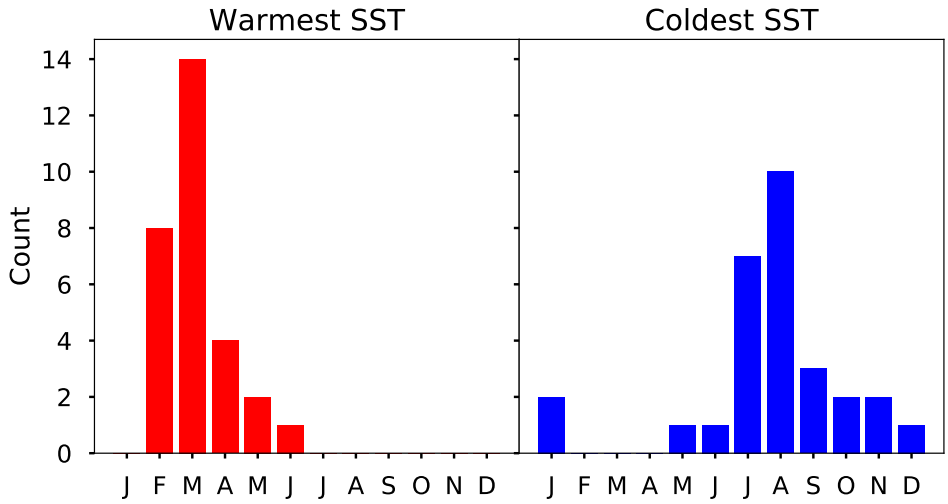

Figure S2. Number of occurrences of warmest (left) and coolest (right) SST during a given month, computed using OISSTv2.

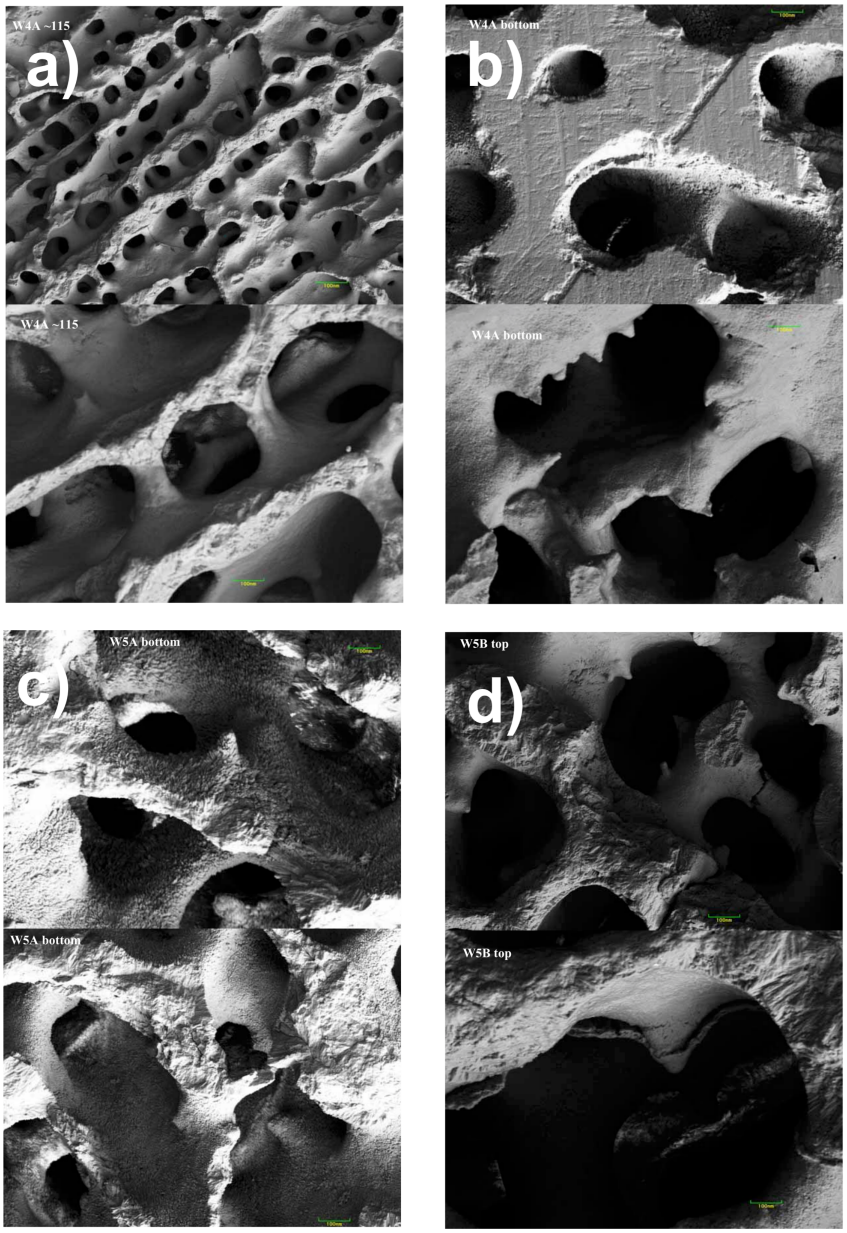

Figure S3. Scanning Electron Microscopy (SEM) images of WLF04 and WLF05, including: a) WLF04 slab A, approximately 115 mm below the top of the core; b) the bottom of WLF04 slab A; c) the bottom of WLF05 slab A; d) the top of WLF05 slab B.

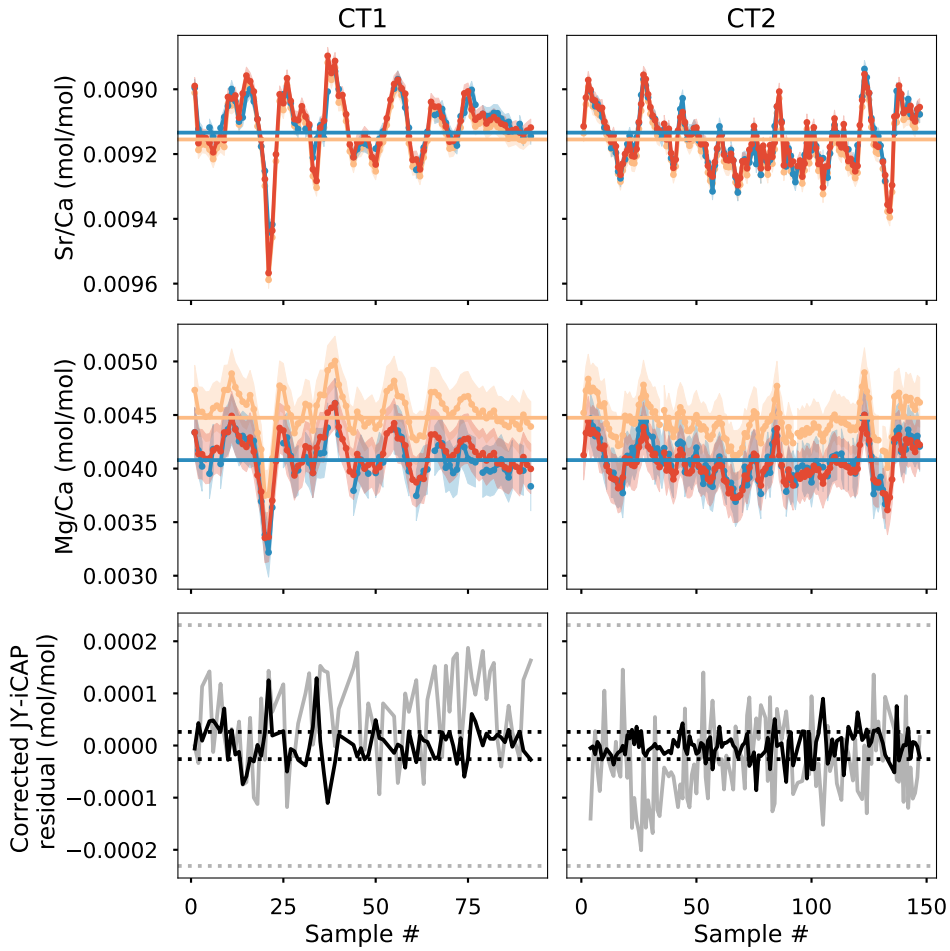

Figure S4. Comparison between the JY and iCAP instruments for WLF04 transects CT1 (left) and CT2 (right). Top row: Sr/Ca for iCAP (blue), original JY (orange), and JY data corrected with a linear offset (red). Analytical precision (1σ) is shaded; horizontal lines denote means (averaged across both CT1 and CT2) of iCAP and original JY data. Middle row: same as top row, but for Mg/Ca. Bottom row: residuals (corrected JY with iCAP subtracted) for Sr/Ca (black) and Mg/Ca (gray), with the 1σ analytical precision for each dataset marked by dotted lines.

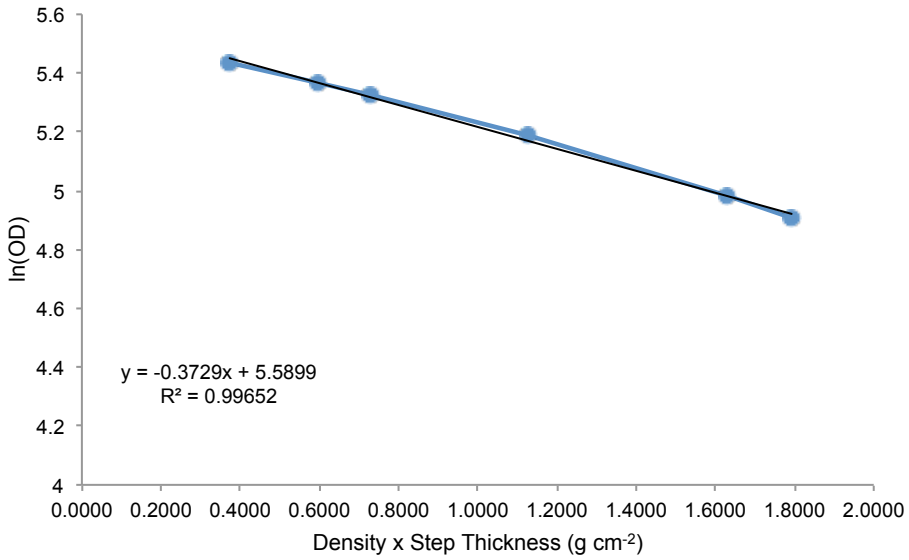

Figure S5. Example X-ray density calibration (from WLF04 slices A-C). The natural log of the optical density (i.e., grayscale value; *y*-axis) is plotted as a function of the product of known density and thickness (*x*-axis) for each standard. A linear regression (black line) is fitted to these standards, and the equation and r^2 value of this line is shown.

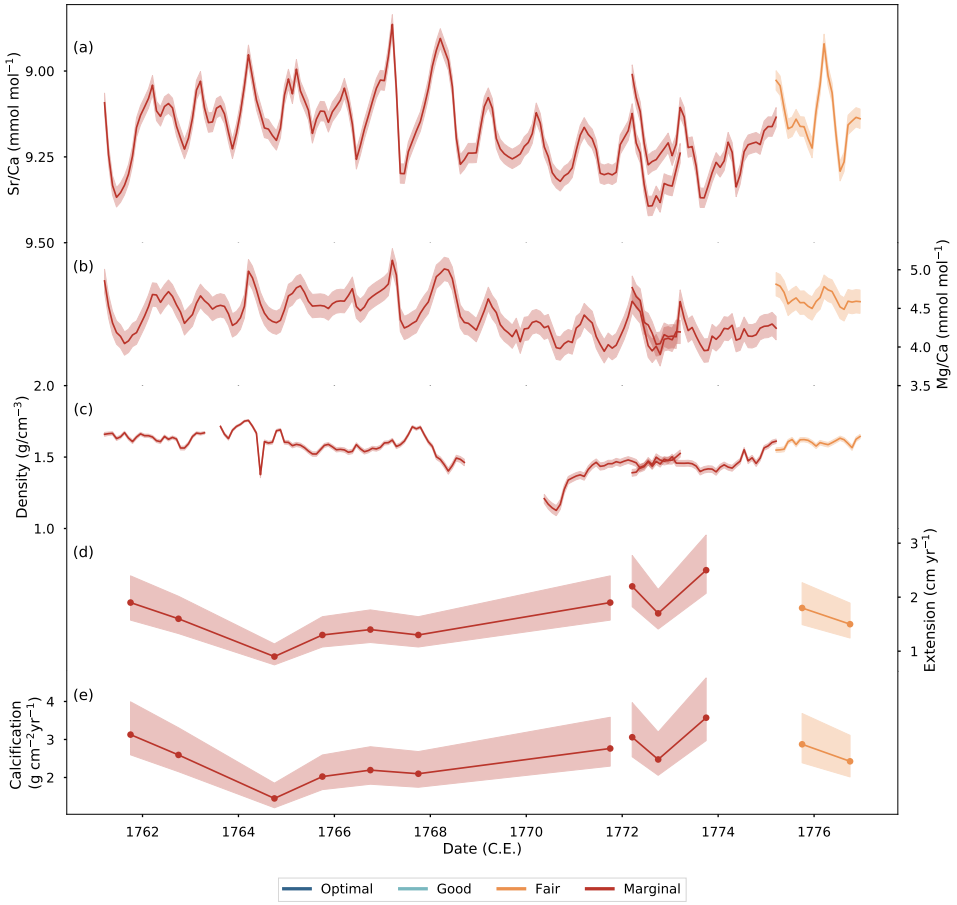

Figure S6. Age-modeled data for all WLF05 transects, including (a) Sr/Ca (y-axis is inverted so warmer SST is upward), (b) Mg/Ca, (c) X-ray density, (d) annual extension rate, and (e) annual calcification rate. Colors denote quality, as in Fig. S7. Shading denotes 1σ uncertainty.

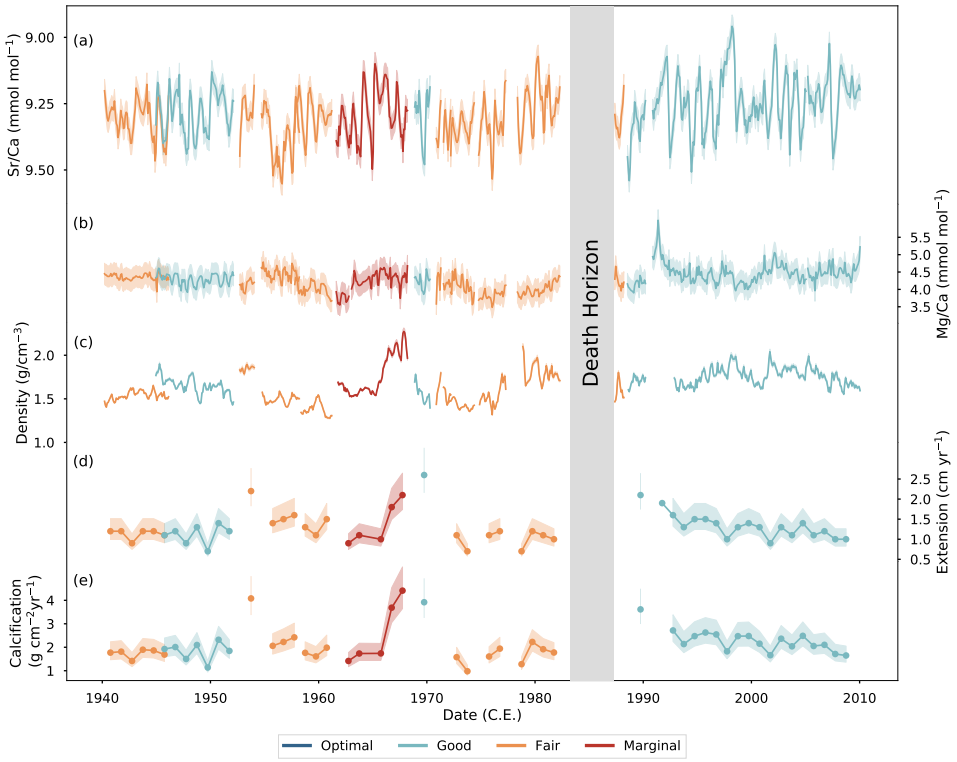

Figure S7. Age-modeled data for all WLF03 transects, including (a) Sr/Ca (y-axis is inverted so warmer SST is upward), (b) Mg/Ca, (c) X-ray density, (d) annual extension rate, and (e) annual calcification rate. Colors denote transect quality from dark blue (optimal) to red (marginal). Shading denotes 1σ uncertainty.

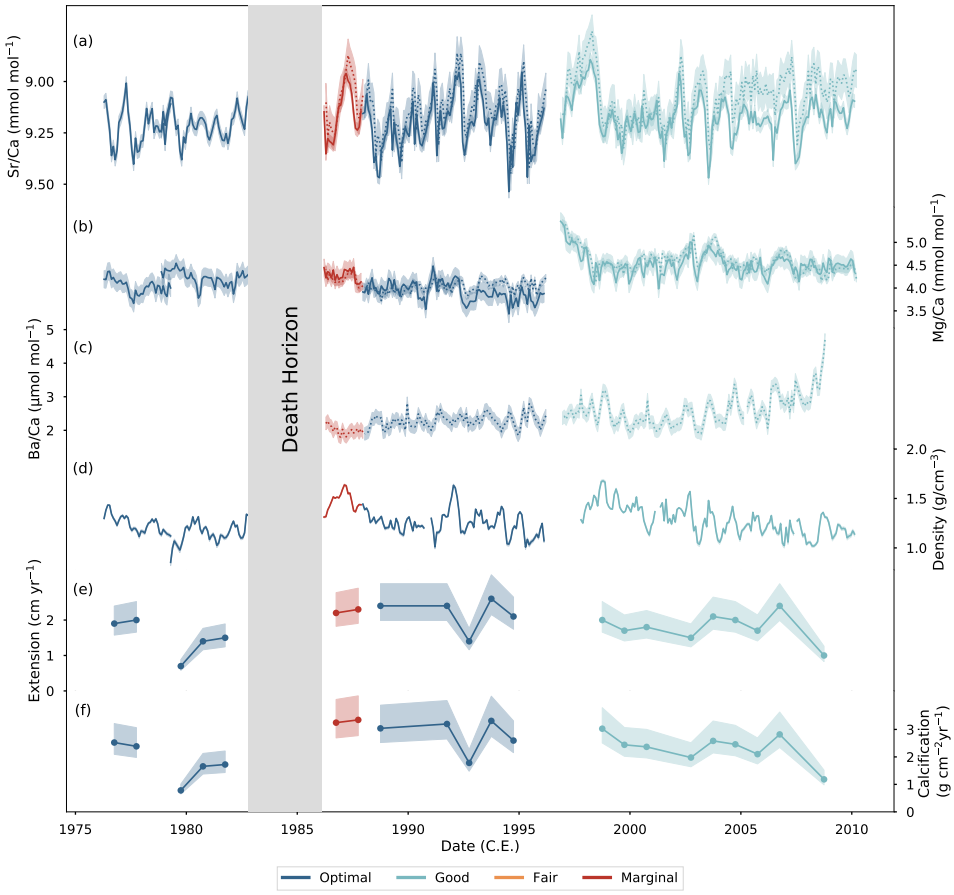

Figure S8. Age-modeled data for all WLF10 transects, including (a) Sr/Ca (y-axis is inverted so warmer SST is upward) from both previously published data (Jimenez *et al.* 2018) (solid lines) and new ICP-OES data run on the same coral powders (Cheung *et al.* in prep.) (dotted lines), (b) Mg/Ca, with published and unpublished data as in (a), (c) Ba/Ca run using ICP-OES (Cheung et al. in prep.), (d) X-ray density, (e) annual extension rate, and (f) annual calcification rate. Colors denote transect quality, as in Fig. S7.

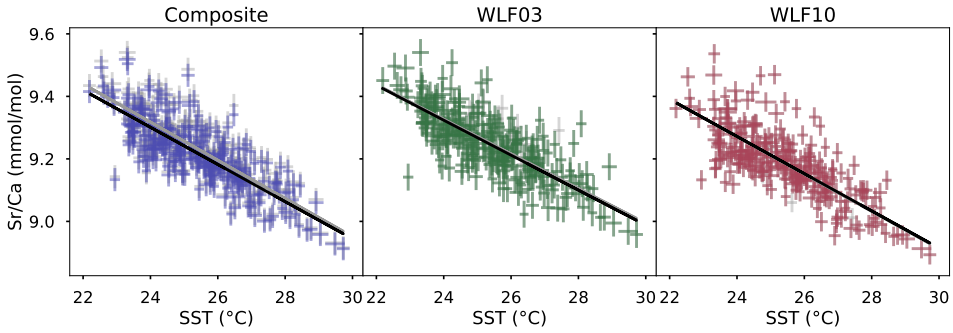

Figure S9. WLS calibration of coral Sr/Ca and OISSTv2 (May 1987-March 2010) for: (a) the composite of WLF03 and WLF10; (b) WLF03; (c) WLF10. All data is given in gray, with a gray line of best fit, and data from high-quality transects only is given in color, with a black line of best fit. Error bars represent Sr/Ca 1σ analytical precision and OISST error. Weighted least squares regression equations and statistics are given in Table S10.

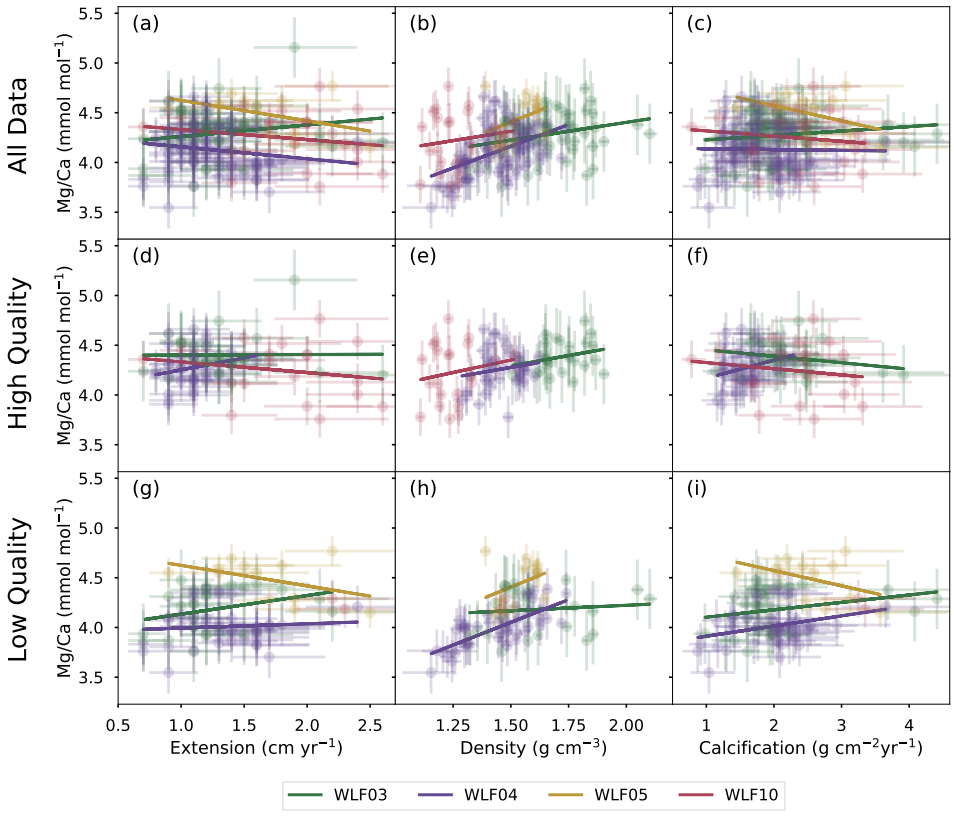

Figure S10. OLS regressions of annual mean Mg/Ca with extension (left), annual mean density (center), and calcification (right) for all corals, including WLF03 (green), WLF04 (purple), WLF05 (yellow), and WLF10 (magenta). 1σ uncertainty is denoted by error bars. (a-c) All data, (d-f) high-quality transects (optimal and good) only, and (g-i) low-quality transects (fair and marginal) only. Regression statistics are given in Table 1.

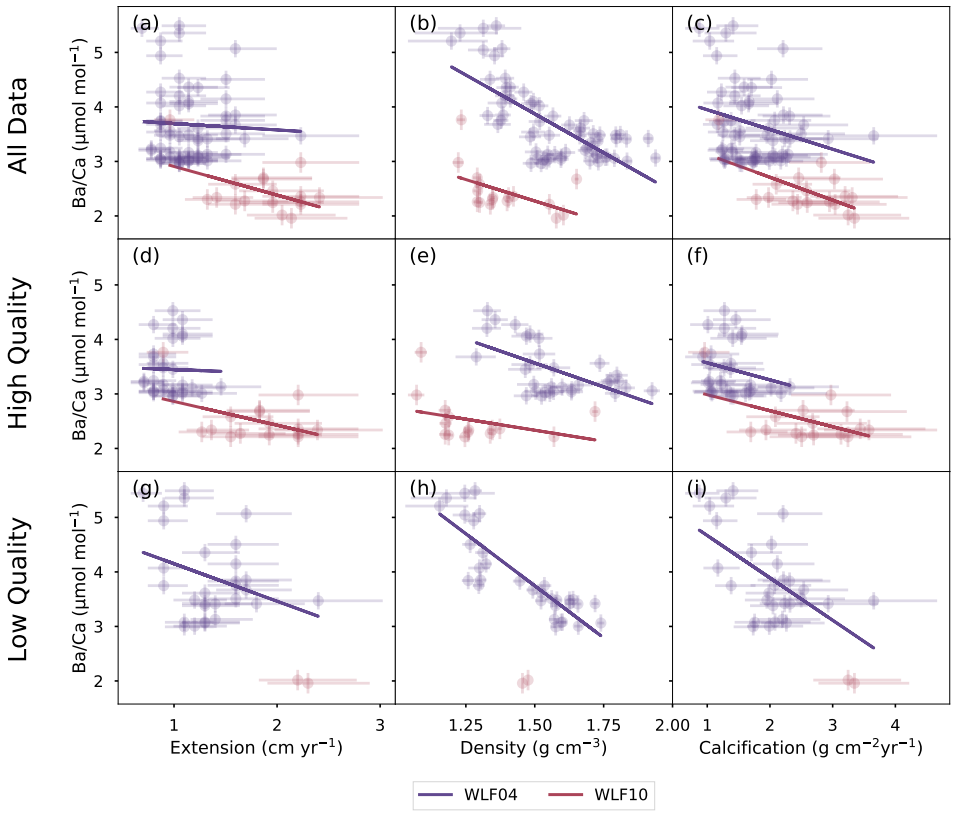

Figure S11. Same as Fig. S10, but for Ba/Ca.

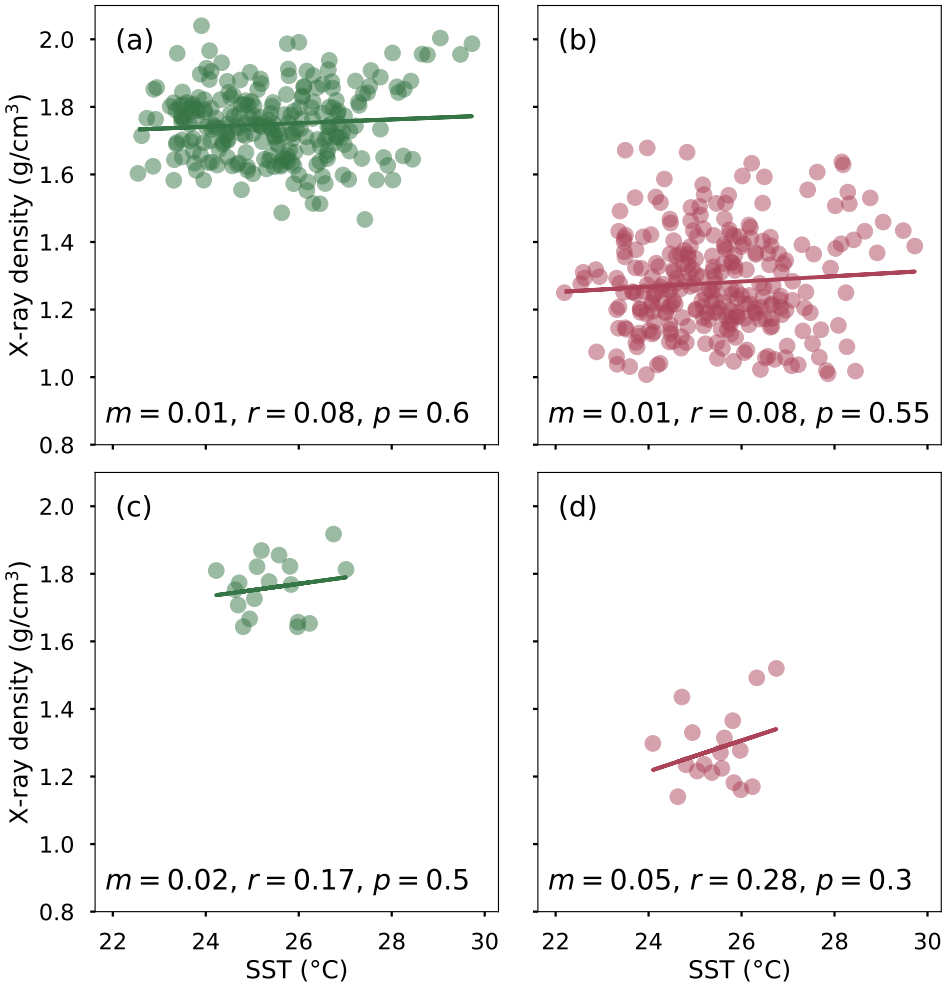

Figure S12. OLS regressions between SST (OISSTv2, 1981-2010) and X-ray density for all qualities of data from modern coral cores, with the slope (m), r-value, and p-value (adjusted for lag-1 autocorrelation) of the regression annotated. Regressions of SST and density for (a) WLF03 on monthly time scales, (b) monthly WLF10, (c) annual WLF03 (including only complete years), and (d) annual WLF10.

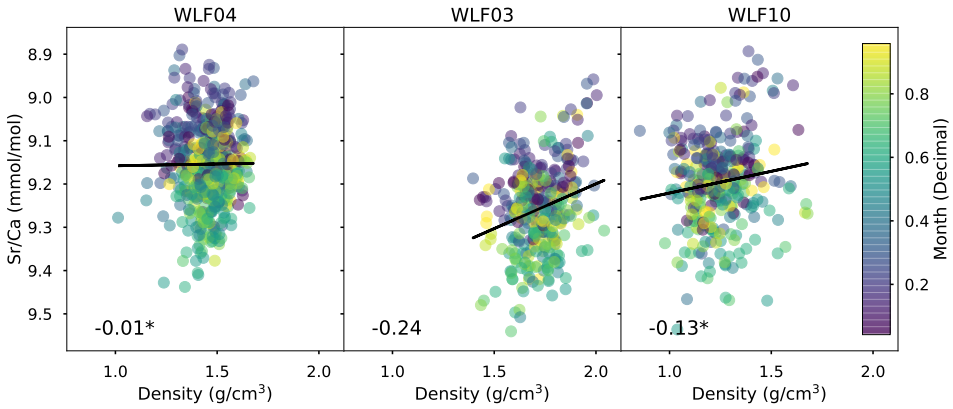

Figure S13. Monthly-resolved scatter plots of X-ray density with Sr/Ca for high-quality data in each core, colored by decimal month (purple=January; yellow=December). Plots are annotated with their corresponding *r*-values; statistical significance ($p \leq 0.05$, after adjusting for lag-1 autocorrelation) is marked with an asterisk.

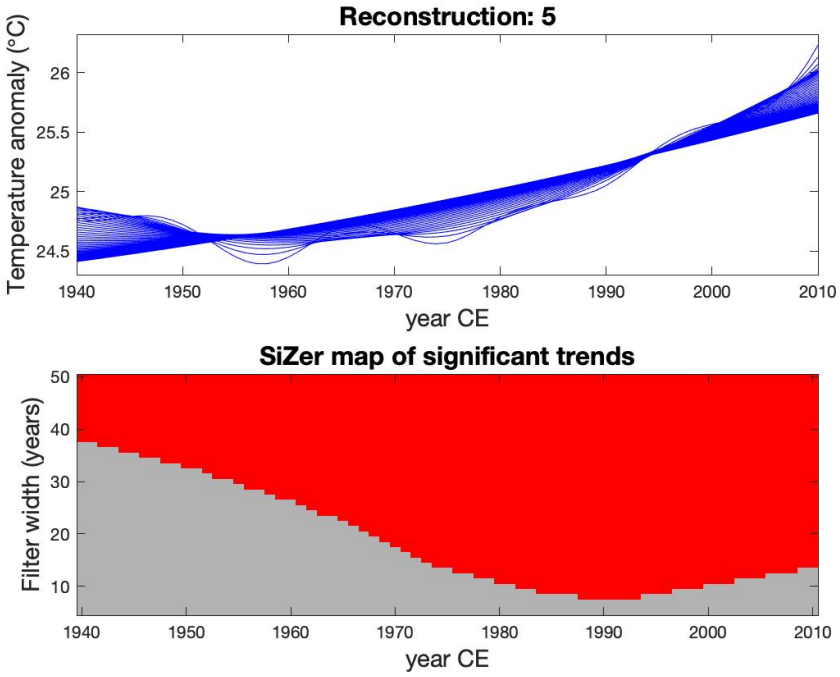

Figure S14. Trend analysis for the composite of WLF03 and WLF10, including all transect qualities. Top: Reconstructed SST smoothed with 5-50 year filters. Bottom: SiZer map showing the presence of significant warming (red), cooling (blue, none present), or no significant trends (light gray) for each year and filter width (significance defined as $p<0.1$).

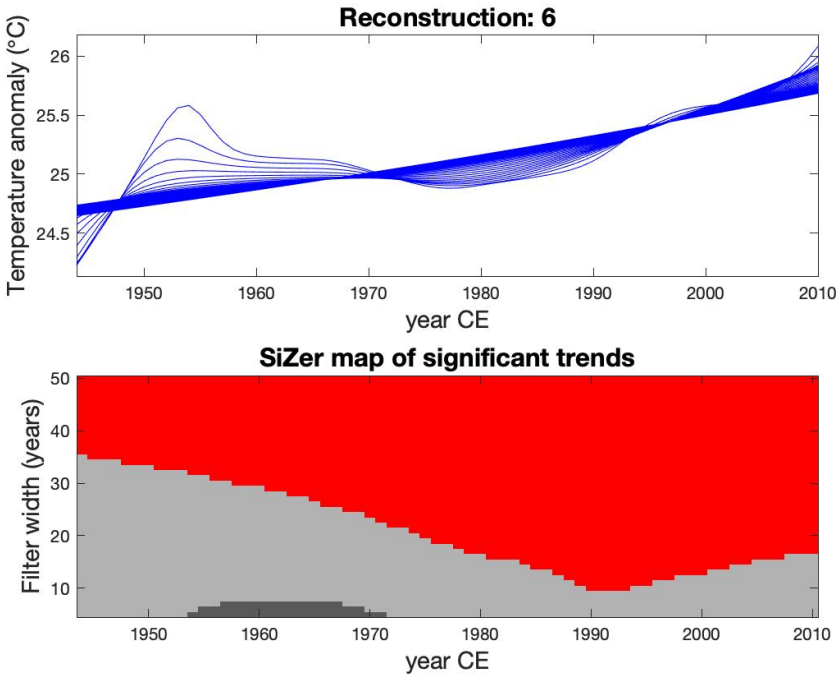

Figure S15. Trend analysis for the composite of WLF03 and WLF10, for high-quality transects only. See Fig. S14 for description. Dark gray shading in the lower panel denotes missing data where low-quality transects were excluded from the SST reconstruction.

Table S1. Description of which instrument, Jobin-Yvon Optima 2c ICP-AES (JY) or Thermo iCAP 7400 series ICP-AES (iCAP) was used for each core or transect. Analytical precision of each trace element is given for each core.

Core	Transect	Instrument	Sr/Ca (mmol/mol)	Mg/Ca (mmol/mol)	Ba/Ca (μmol/mol)
WLF03	-	JY	± 0.043	± 0.304	-
WLF04	AT1	JY	± 0.026	± 0.212	± 0.159
	AT2	iCAP			
	BT4	iCAP			
	BT1	JY			
	BT2	iCAP			
	BT3	JY			
	CT1	iCAP (with JY for comparison)			
	CT2	iCAP (with JY for comparison)			
	DT2	iCAP			
	FT0	iCAP			
	FT1	iCAP			
	FT2	iCAP			
	FT3	iCAP			
	GT1	iCAP			
WLF05	-	JY	± 0.028	± 0.151	-
WLF10	-	JY (Mg/Ca and Sr/Ca) & iCAP (Ba/Ca)	± 0.031	± 0.189	± 0.188

Table S2. U/Th ages for fossil cores WLF04 and WLF05. *$\delta^{234}U$ = ([$^{234}U/^{238}U$]activity - 1)x1000. ** $\delta^{234}U_{initial}$ was calculated based on ^{230}Th age (*T*), i.e., $\delta^{234}U_{initial}$ = $\delta^{234}U_{measured}$ x el234 x *T*. Corrected 230Th ages assume the initial $^{230}Th/^{232}Th$ atomic ratio of 4.4±2.2 x10^{-6}. Those are the values for a material at secular equilibrium, with the bulk earth $^{232}Th/^{238}U$ value of 3.8. The errors are arbitrarily assumed to be 50%. ***B.P. stands for "Before Present" where the "Present" is defined as the January 1, 1950 C.E.. All errors are ±2σ.

Core	^{238}U (ppb)	^{232}Th (ppt)	^{230}Th / ^{232}Th (atomic x10^{-6})	$\delta^{234}U$* (measured)	^{230}Th / ^{238}U (activity)	^{230}Th Age (yr) (uncorrected)	^{230}Th Age (yr) (corrected)	$\delta^{234}U$Initial** (corrected)	^{230}Th Age (yr BP)*** (corrected)
WLF04	2567±6	36±3	3479±298	145±3	0.0029±0.0001	281±7	280±7	145±3	218±7
WLF05	2315±3	74±2	1482±54	147±2	0.0029±0.0001	275±5	274±5	147±2	212±5

Table S3. Qualities of each transect (1=optimal, 4=marginal), with justification.

Core	Name	Quality	Notes
WLF03	AT1	2	changes in growth direction; weak density banding
WLF03	BT1	2	slightly off-axis
WLF03	BT2	3	changes in growth direction; slightly off-axis
WLF03	CT1	4	changes in growth direction; disorganized growth; weak growth bands
WLF03	CT2a	3	changes in growth direction; slightly off-axis
WLF03	CT2b	3	changes in growth direction; slightly off-axis
WLF03	CT3	3	angled corallites; disorganized growth
WLF03	DT1	3	off-axis corallites; weak density banding
WLF03	DT2	3	changes in growth direction; corallites slightly off-axis
WLF03	DT3	2	on-axis, clear density bands
WLF03	DT4	4	in growth trough
WLF03	D2T1	3	corallites angled relative to transect
WLF03	D2T2	3	corallites angled relative to transect; off-axis corallites
WLF03	ET1a	2	corallites angled relative to transect; changes in growth direction
WLF03	ET1b	3	corallites angled relative to transect; changes in growth direction; off-axis corallites
WLF03	ET2	2	changes in growth direction
WLF04	AT1	3	suspected diagenesis near top; small changes in growth direction; weak density banding
WLF04	AT2	2	weak density banding
WLF04	BT1	4	angled corallites; changes in growth direction; approaches trough
WLF04	BT2	2	weak density banding
WLF04	BT3a	3	strongly angled corallites
WLF04	BT3b	2	weakly angled corallites
WLF04	BT4	2	weak density banding
WLF04	CT1	4	angled corallites; changes in growth direction; weak density banding
WLF04	CT2	4	strongly angled corallites; weak density banding
WLF04	DT2a	4	angled corallites and weak banding
WLF04	DT2b	1	clear, parallel growth bands
WLF04	FT0	4	angled corallites; changes in growth direction
WLF04	FT1a	4	strongly angled corallites
WLF04	FT1b	2	on-axis, but weak density banding
WLF04	FT2a	3	angled corallites; changes in growth direction
WLF04	FT2b	2	small changes in growth direction
WLF04	FT3	2	weak density banding
WLF04	GT1a	2	small changes in growth direction
WLF04	GT1b	4	changes in growth direction; corallites off-axis
WLF05	AT1	3	suspected diagenesis near top; weak density banding; off-axis corallites
WLF05	AT2	4	strongly angled corallites
WLF05	BT1	4	strongly angled corallites; changes in growth direction
WLF10	AT1	2	small changes in growth direction; some regions with low density banding
WLF10	BT1a	1	regular, clear growth bands; parallel corallites
WLF10	BT1b	4	high-density bands adjacent to death horizon
WLF10	CT1	1	regular, clear growth bands; parallel corallites
WLF10	CT2	1	regular, clear growth bands; parallel corallites

Table S4. Comparison of X-ray and gamma density for available cores (WLF04 and WLF05). All units are in g cm^{-3}.

	Mean	Median	Std. Dev.	Variance	Minimum	Maximum	Count
WLF04 Gamma	1.36	1.37	0.13	0.02	1.06	1.65	1066
WLF04 X-ray	1.45	1.47	0.13	0.02	1.01	1.78	1066
WLF05 Gamma	1.45	1.46	0.10	0.01	0.99	1.67	179
WLF05 X-ray	1.53	1.56	0.11	0.01	1.13	1.76	179

Table S5. Summary statistics for Sr/Ca (mmol/mol) for all coral records, grouped by quality. For WLF03, WLF04, and WLF10, quality show a statistically significant difference (Kruskal-Wallis $p \leq 0.01$); for WLF05, no quality groups are significantly different. Groups are determined using a Dunn's post-hoc test; shared groups (Dunn's test $p \geq 0.05$) are listed in the final column.

	Mean	Median	Std. Dev.	Variance	Minimum	Maximum	# Months	Group
WLF03 1 (Optimal)	-	-	-	-	-	-	-	
WLF03 2 (Good)	9.26	9.26	0.1	0.01	8.96	9.54	356	
WLF03 3 (Fair)	9.31	9.31	0.08	0.01	9.07	9.55	306	4
WLF03 4 (Marginal)	9.29	9.3	0.1	0.01	9.1	9.5	78	3
WLF04 1 (Optimal)	9.16	9.16	0.09	0.01	8.97	9.44	106	2, 4
WLF04 2 (Good)	9.15	9.15	0.1	0.01	8.89	9.41	508	1
WLF04 3 (Fair)	9.21	9.21	0.1	0.01	8.96	9.46	145	
WLF04 4 (Marginal)	9.17	9.17	0.1	0.01	8.89	9.44	511	1
WLF05 1 (Optimal)	-	-	-	-	-	-	-	
WLF05 2 (Good)	-	-	-	-	-	-	-	
WLF05 3 (Fair)	9.13	9.14	0.09	0.01	8.92	9.29	22	
WLF05 4 (Marginal)	9.18	9.19	0.1	0.01	8.86	9.39	182	
WLF10 1 (Optimal)	9.21	9.21	0.1	0.01	8.95	9.54	183	4
WLF10 2 (Good)	9.17	9.17	0.1	0.01	8.89	9.47	160	4
WLF10 3 (Fair)	-	-	-	-	-	-	-	
WLF10 4 (Marginal)	9.16	9.15	0.12	0.01	8.96	9.35	21	1, 2

Table S6. Same as Table S5, but for Mg/Ca (mmol/mol). For all cores, Kruskal-Wallis $p \leq 0.01$.

	Mean	Median	Std. Dev.	Variance	Minimum	Maximum	# Months	Group
WLF03 1 (Optimal)	-	-	-	-	-	-	-	
WLF03 2 (Good)	4.4	4.39	0.27	0.07	3.86	5.99	356	
WLF03 3 (Fair)	4.16	4.2	0.26	0.07	3.48	4.79	306	4
WLF03 4 (Marginal)	4.21	4.24	0.29	0.08	3.55	4.68	76	3
WLF04 1 (Optimal)	4.14	4.18	0.21	0.05	3.58	4.65	106	
WLF04 2 (Good)	4.3	4.28	0.28	0.08	3.61	5.14	508	
WLF04 3 (Fair)	4	3.96	0.22	0.05	3.58	4.81	145	4
WLF04 4 (Marginal)	3.99	3.99	0.27	0.07	3.28	4.74	503	3
WLF05 1 (Optimal)	-	-	-	-	-	-	-	
WLF05 2 (Good)	-	-	-	-	-	-	-	
WLF05 3 (Fair)	4.62	4.59	0.09	0.01	4.49	4.81	22	
WLF05 4 (Marginal)	4.38	4.33	0.26	0.07	3.9	5.12	182	
WLF10 1 (Optimal)	4.02	4.03	0.22	0.05	3.43	4.54	183	
WLF10 2 (Good)	4.53	4.51	0.24	0.06	3.98	5.46	160	
WLF10 3 (Fair)	-	-	-	-	-	-	-	
WLF10 4 (Marginal)	4.28	4.29	0.12	0.01	4.09	4.46	21	

Table S7. Same as Table S5, but for Ba/Ca (μmol/mol). For WLF04 and WLF10, Kruskal-Wallis $p \leq 0.01$.

	Mean	Median	Std. Dev.	Variance	Minimum	Maximum	# Months	Group
WLF03 1 (Optimal)	-	-	-	-	-	-	-	
WLF03 2 (Good)	-	-	-	-	-	-	-	
WLF03 3 (Fair)	-	-	-	-	-	-	-	
WLF03 4 (Marginal)	-	-	-	-	-	-	-	
WLF04 1 (Optimal)	4.17	4.09	0.4	0.16	3.63	5.84	106	
WLF04 2 (Good)	3.29	3.17	0.45	0.2	2.63	5.93	363	
WLF04 3 (Fair)	5.96	6	0.94	0.88	4.23	7.41	25	
WLF04 4 (Marginal)	3.97	3.68	0.88	0.77	2.74	9.08	451	
WLF05 1 (Optimal)	-	-	-	-	-	-	-	
WLF05 2 (Good)	-	-	-	-	-	-	-	
WLF05 3 (Fair)	-	-	-	-	-	-	-	
WLF05 4 (Marginal)	-	-	-	-	-	-	-	
WLF10 1 (Optimal)	2.28	2.27	0.2	0.04	1.86	2.81	98	
WLF10 2 (Good)	2.6	2.52	0.47	0.22	1.9	4.69	141	
WLF10 3 (Fair)	-	-	-	-	-	-	-	
WLF10 4 (Marginal)	2	1.98	0.13	0.02	1.79	2.28	21	

Table S8. Same as Table S5, but for X-ray density (g cm^{-3}). For all cores, Kruskal-Wallis $p \leq 0.01$.

	Mean	Median	Std. Dev.	Variance	Minimum	Maximum	# Months	Group
WLF03 1 (Optimal)	-	-	-	-	-	-	-	
WLF03 2 (Good)	1.72	1.71	0.12	0.01	1.4	2.04	332	4
WLF03 3 (Fair)	1.56	1.52	0.16	0.03	1.28	2.1	293	
WLF03 4 (Marginal)	1.77	1.66	0.23	0.05	1.52	2.27	76	2
WLF04 1 (Optimal)	1.35	1.36	0.08	0.01	1.01	1.49	84	
WLF04 2 (Good)	1.47	1.48	0.09	0.01	1.16	1.68	427	3
WLF04 3 (Fair)	1.46	1.47	0.05	0	1.32	1.59	119	2, 4
WLF04 4 (Marginal)	1.43	1.43	0.17	0.03	1.1	1.78	489	3
WLF05 1 (Optimal)	-	-	-	-	-	-	-	
WLF05 2 (Good)	-	-	-	-	-	-	-	
WLF05 3 (Fair)	1.6	1.6	0.03	0	1.55	1.64	22	
WLF05 4 (Marginal)	1.53	1.54	0.12	0.01	1.13	1.76	160	
WLF10 1 (Optimal)	1.22	1.21	0.12	0.01	0.85	1.63	175	
WLF10 2 (Good)	1.28	1.26	0.15	0.02	1.02	1.68	146	
WLF10 3 (Fair)	-	-	-	-	-	-	-	
WLF10 4 (Marginal)	1.47	1.47	0.09	0.01	1.31	1.64	21	

Table S9. Slope (m), intercept (b), and r^2, with significance marked by * (autocorrelation-adjusted $p \leq 0.10$), ** (autocorrelation-adjusted $p \leq 0.05$), and † (un-adjusted $p \leq 0.05$), for OLS regressions between annual growth metrics and trace elemental ratios. Results are shown for all transect qualities ("All"), high-quality only ("HQ"), and low-quality only ("LQ"). Results with small sample sizes ($n \leq 3$) are not included.

			WLF03			WLF04			WLF05			WLF10		
x	*y*	Quality	*m*	*b*	r^2	*m*	*b*	r^2	*m*	*b*	r^2	*m*	*b*	r^2
Extension	Sr/Ca	All	0.012	9.266	0.01	-0.022	9.188	0.01	0.069	9.031	0.16*	-0.007	9.206	0.01
		HQ	0.030	9.216	0.04	-0.063	9.212	0.05				0.000	9.196	0.00
		LQ	0.007	9.300	0.00	-0.051	9.243	0.06	0.069	9.031	0.16			
Density	Sr/Ca	All	-0.186	9.591	0.24*†	-0.229	9.499	0.19†	-0.234	9.523	0.06	-0.168	9.407	0.18*†
		HQ	-0.236	9.661	0.16†	-0.089	9.282	0.02				-0.167	9.405	0.14*
		LQ	-0.127	9.512	0.21†	-0.258	9.550	0.3†	-0.234	9.523	0.06			
Calcification	Sr/Ca	All	-0.003	9.290	0.00	-0.029	9.211	0.05	0.057	9.000	0.20**	-0.013	9.223	0.04
		HQ	0.021	9.212	0.04	-0.051	9.225	0.08				-0.006	9.211	0.01
		LQ	-0.008	9.325	0.01	-0.048	9.267	0.14†	0.057	9.000	0.20			
Extension	Mg/Ca	All	0.117	4.143	0.03	-0.120	4.277	0.02	-0.206	4.830	0.19**	-0.102	4.433	0.03
		HQ	0.005	4.397	0.00	0.241	4.012	0.05				-0.107	4.440	0.03
		LQ	0.187	3.947	0.09	0.043	3.951	0.01	-0.206	4.830	0.19			
Density	Mg/Ca	All	0.357	3.689	0.08†	0.871	2.856	0.23†	0.949	2.982	0.13	0.374	3.752	0.02
		HQ	0.414	3.672	0.07	0.404	3.671	0.03				0.502	3.599	0.03
		LQ	0.109	4.004	0.01	0.913	2.682	0.54†	0.949	2.982	0.13			
Calcification	Mg/Ca	All	0.045	4.182	0.02	-0.008	4.146	0.00	-0.153	4.878	0.18*	-0.052	4.370	0.02
		HQ	-0.065	4.519	0.06	0.181	3.987	0.07				-0.062	4.387	0.02
		LQ	0.075	4.029	0.07	0.102	3.810	0.09	-0.153	4.878	0.18			
Extension	Ba/Ca	All				-0.106	3.805	0.00				-0.476	3.405	0.24*†
		HQ				-0.067	3.521	0.00				-0.407	3.314	0.20
		LQ				-0.689	4.839	0.09						
Density	Ba/Ca	All				-3.610	8.904	0.52†				-1.990	5.047	0.24†
		HQ				-3.344	8.246	0.35†				-1.546	4.498	0.12
		LQ				-3.816	9.469	0.73†						
Calcification	Ba/Ca	All				-0.362	4.310	0.07†				-0.420	3.549	0.36**†
		HQ				-0.384	4.037	0.05				-0.361	3.425	0.26
		LQ				-0.777	5.445	0.33†						
Density	Extension	All	0.361	0.672	0.03	0.356	0.698	0.02	-3.162	6.557	0.42*†	1.747	-0.377	0.16*
		HQ	-1.168	3.31	0.10	0.177	0.824	0.01				1.597	-0.195	0.10
		LQ	0.728	0.075	0.16*†	0.422	0.720	0.04	-3.162	6.557	0.42*†			

Table S10. Statistics for all Sr/Ca-SST calibrations, obtained from WLS regression of Sr/Ca vs. OISSTv2 over the interval of May 1987-March 2010.

	Slope	Intercept	r^2	RMSE
Composite (all)	-0.061 ± 0.002	10.783 ± 0.040	0.69	0.066
Composite (high quality)	-0.059 ± 0.002	10.728 ± 0.040	0.69	0.064
WLF03 (all)	-0.055 ± 0.002	10.656 ± 0.047	0.61	0.068
WLF03 (high quality)	-0.056 ± 0.002	10.666 ± 0.047	0.63	0.067
WLF10 (all)	-0.060 ± 0.001	10.706 ± 0.035	0.65	0.071
WLF10 (high quality)	-0.060 ± 0.001	10.700 ± 0.035	0.65	0.072

Table S11. Root mean squared errors (RMSE) (°C) between ERSSTv5 (1950-2010) and reconstructed SST of modern corals, reconstructed using Sr/Ca of only high-quality transects, with both high- and all-quality Sr/Ca-SST calibrations applied. Sample sizes are given in parentheses.

	Composite (high-quality)	WLF03 (high-quality)	WLF10 (high-quality)
All data calibration	1.19 (390)	1.37 (295)	1.31 (337)
High-quality only calibration	1.31 (390)	1.38 (295)	1.31 (337)

References

Cantarero, S. I., J. T. Tanzil, and N. F. Goodkin (2017), Simultaneous analysis of Ba and Sr to Ca ratios in scleractinian corals by inductively coupled plasma optical emissions spectrometry, *Limnology and Oceanography: Methods*, *15*(1), 116–123, doi: 10.1002/lom3.10152.

Chalker, B. E., and D. J. Barnes (1990), Gamma densitometry for the measurement of skeletal density, *Coral Reefs*, *9*(1), 11–23, doi:10.1007/BF00686717.

Hathorne, E. C., A. Gagnon, T. Felis, J. Adkins, R. Asami, W. Boer, N. Caillon, D. Case, K. M. Cobb, E. Douville, P. Demenocal, A. Eisenhauer, D. Garbe-Schönberg, W. Geibert, S. Goldstein, K. Hughen, M. Inoue, H. Kawahata, M. Kölling, F. L. Cornec, B. K. Linsley, H. V. McGregor, P. Montagna, I. S. Nurhati, T. M. Quinn, J. Raddatz, H. Rebaubier, L. Robinson, A. Sadekov, R. Sherrell, D. Sinclair, A. W. Tudhope, G. Wei, H. Wong, H. C. Wu, and C. F. You (2013), Interlaboratory study for coral Sr/Ca and other element/Ca ratio measurements, *Geochemistry, Geophysics, Geosystems*, *14*(9), 3730–3750, doi: 10.1002/ggge.20230.

Jimenez, G., J. E. Cole, D. M. Thompson, and A. W. Tudhope (2018), Northern Galápagos Corals Reveal Twentieth Century Warming in the Eastern Tropical Pacific, *Geophysical Research Letters*, *45*(4), 1981–1988, doi:10.1002/2017GL075323.

Kessler, W. S. (2006), The circulation of the eastern tropical Pacific: A review, *Progress in Oceanography*, *69*(2-4), 181–217, doi:10.1016/j.pocean.2006.03.009.

Ku, H.H. (1966), Notes on the use of propagation of error formulas, *Journal of Research of the National Bureau of Standards. Section C: Engineering and Instrumentation*, *70C*(4), 263–273, doi:10.6028/jres.070C.025.

Schindelin, J., I. Arganda-Carreras, E. Frise, V. Kaynig, M. Longair, T. Pietzsch, S. Preibisch, C. Rueden, S. Saalfeld, B. Schmid, J.-Y. Tinevez, D. J. White, V. Hartenstein, K. Eliceiri, P. Tomancak, and A. Cardona (2012), Fiji: an open-source platform for biological-image analysis, *Nature Methods*, *9*(7), 676–682, doi:10.1038/nmeth.2019.

Schrag, D. P. (1999), Rapid analysis of high-precision Sr/Ca ratios in corals and other marine carbonates, *Paleoceanography*, *14*(2), 97–102.

Shen, G., J. Cole, D. Lea, L. Linn, T. Mcconnaughey, and R. Fairbanks (1992), Surface ocean variability at Galapagos from 1936-1982: Calibration of geochemical tracers in corals, *October*, *7*(5), 563–588.